Elevation plane spatial multicell interference mitigation with No CSI sharing

Elevation Plane Spatial Multicell Interference Mitigation With no CSI Sharing

Nima Seifi*, Mikael Coldrey†, and Tommy Svensson‡
Ericsson Research, *SE-164 80 Stockholm and †SE-417 56 Gothenburg, Sweden
‡Dept. of Signals and Systems, Chalmers University of Technology, SE-412 96 Gothenburg, Sweden
Email: *nima.seifi@ericsson.com, †mikael.coldrey@ericsson.com, ‡tommy.svensson@chalmers.se

***Abstract*—We study downlink transmission in a cellular network with multi-antenna base stations (BSs) and single-antenna users. We propose a novel coordinated transmission strategy that controls the intercell interference (ICI) via exploiting the elevation plane of the wireless channel. The key idea is to divide the area of each cell into two disjoint vertical regions and to serve the non-adjacent vertical regions in the neighboring cells according to a set of *pre-determined coordinated transmission patterns*. A scheduler is used to dynamically allocate the available time-slots among transmission patterns. By appropriately adapting the elevation angle of the antenna main beam, denoted as tilt, at the BSs in each pattern, ICI can be effectively suppressed. Unlike the state-of-the-art coordinated transmission schemes, the proposed technique requires no channel state information sharing among BSs and/or infeasible BS tilting capabilities, but achieves comparable performance.**

I. Introduction

Fifth generation of cellular systems (5G) is expected to provide ubiquitous high data-rate coverage and seamless user experience for large and diverse sets of devices. Achieving this target in future ultra dense networks with universal frequency reuse needs advanced intercell interference (ICI) management [1]. As one efficient approach to address this issue, base station (BS) coordination techniques have been under investigation over the last years [2]. The required signaling overhead and complexity of these techniques, however, has prevented their acceptance to the standard so far.

Coordinated beamforming is one form of BS coordination that mitigates the ICI via joint beamforming design at the BSs. Prior work on coordinated beamforming mainly builds upon channel state information (CSI) sharing among the BSs, thereby imposing significant signaling overhead on the network. Moreover, this work has mostly considered 2D cellular layouts and investigated the ICI management gains in the azimuth plane of the wireless channel (see e.g., [3] and references therein). Promised gains of the proposed techniques are also highly sensitive to the CSI imperfections (error, delay, etc.) incurred in the feedback and/or backhaul links [3], [4].

Another simple and efficient approach for ICI management is to exploit the elevation plane of the wireless channel. For example, by adapting the elevation angle of the BS antenna main beam, denoted as *tilt*, each BS can increase the desired signal level to/from a user in its own cell and/or to reduce the ICI leakage to/from the users in the neighboring cells [5]. The BS tilt can be adjusted electronically by changing the phase of the antenna excitation in the analog or digital domain, thereby enabling fast tilt adaptation at the BSs. Recently, coordinated beamforming strategies exploiting dynamic tilt adaptation has attracted a lot of interest as these strategies do not need instantaneous CSI sharing among the BSs [4], [6]–[8]. The proposed techniques mainly assume accurate knowledge of users' elevation angles at all BSs [4], [6]–[8], which is very difficult to obtain in practice. Moreover, some of these techniques [4], [7] further needs each BS to change its tilt continuously from 0° to 90°. Such BS tilting capability requires infeasibly large antenna arrays. To address these difficulties, a so-called implicit coordination method was proposed in [8] in which the ICI mitigation is achieved by combining tilt switching with static allocation of available frequency (or time) resources among sectors within each cell and by ensuring that the equivalent vertical sectors at neighboring cells are served over orthogonal resources. Such static allocation of resources might be a suitable strategy for densely populated networks, but can result in performance loss in networks with low to moderate number of users per cell.

In this paper, we focus on a cellular network with low to moderate number of users per cell. We propose a novel coordinated transmission strategy in which the ICI is mitigated solely in the elevation plane of the wireless channel. In the proposed technique, the area of each cell is divided into two disjoint vertical regions, namely, the cell-interior region and the cell-edge region. The non-adjacent vertical regions in the neighboring cells are then served according to a set of *pre-determined coordinated transmission patterns* such that in each pattern only one BS is allowed to schedule its cell-edge region for transmission. The available time-slots are *dynamically* allocated to different patterns depending on the number of users in all the vertical regions. By applying optimized tilts at the BSs, the ICI at the scheduled cell-edge region can be sufficiently mitigated with no need for neither CSI or users' elevation angles sharing among BSs nor infeasible BS tilting capabilities.

Notation: Vectors and matrices are denoted by bold-face lower-case and upper-case letters, respectively. $(\cdot)^{\mathsf{H}}$ is the complex conjugate transpose. $|\mathcal{S}|$ denotes the cardinality of a set $\mathcal{S}$. $\|\boldsymbol{x}\|$ is the Euclidean norm of a complex vector $\boldsymbol{x}$.

II. System Model

We consider downlink transmission in a network consisting of B mutually interfering cells that are uniquely indexed as $b = 1, \ldots, B$. Each cell has a multi-antenna BS located at a height h_{bs} above the ground. There are K_b users uniformly distributed in cell b, $\forall b$, each at a height h_{u} above the ground and equipped with a single antenna. We assume an intracell orthogonal multiple access technique such that each BS serves only one user per time-frequency resource block in its own

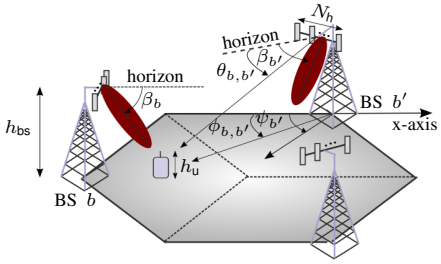

Fig. 1. An example of a 3-cell network with illustration of spherical angles.

cell, denoted as the *active* user, while causing ICI to the neighboring cells. We denote the active user and its serving BS in cell b as user b and BS b, respectively. An example of a network consisting of three romb-shaped cells is shown in Fig. 1. We use this configuration as an instructive example in this paper because it is a relevant setup in cellular networks with hexagonal cell layout and 120° cell sectoring.

A. Propagation Environment

We focus on a typical urban non-line-of-sight (NLOS) propagation scenario in which the BSs are deployed at a height much greater than the large-scale clutter, such as buildings and trees, and the users are located close to the ground (i.e., $h_{\mathsf{u}} \ll h_{\mathsf{bs}}$) and dipped in the clutter. In such a propagation environment, the transmitted signal from the BS most likely experiences a rich scattering in the azimuth plane, while it undergoes only few reflections and diffractions in the elevation plane. Here, to simplify the propagation channel modeling, we assume that multipath fading is rich in the horizontal plane, while it is negligible in the elevation plane. Although not fully realistic in a NLOS environment, recent measurements have shown that this is a reasonable assumption when the BS is located high above the rooftop as assumed in this paper [9].

B. Antenna Configuration

We assume a 3D unity-gain isotropic antenna at the user. At the BS, we consider an array of N_{h} antennas that are arranged in a horizontal plane parallel to the ground. Each BS antenna itself comprises multiple vertically stacked radiating elements that are contained within a radome. The radiation pattern of each antenna depends on the number of radiating elements, their radiation patterns, their relative positions, and their applied weights. By applying appropriate weights it is possible to control the elevation characteristics of the antenna radiation pattern including the tilt. Here, to enable an abstraction of the role played by the radiating elements in controlling the tilt, we approximate each BS antenna pattern using the 3D directional model proposed in 3GPP [10]. According to this model, the observed antenna gain from any antenna of BS b' at user b is expressed in dBi scale as

$$G^{\mathsf{dBi}}_{b,b'}(\beta_{b'}) = -\min\left[12\left(\frac{\phi_{b,b'}-\psi_{b'}}{\phi^{\mathsf{3dB}}_{b'}}\right)^2, \mathrm{SLL}_{\mathsf{az}}\right] - \min\left[12\left(\frac{\theta_{b,b'}-\beta_{b'}}{\theta^{\mathsf{3dB}}_{b'}}\right)^2, \mathrm{SLL}_{\mathsf{el}}\right]. \quad (1)$$

In (1), $\phi_{b,b'}$ is the azimuth angle measured between the line in the azimuth plane connecting user b to BS b' and the array boresight of BS b', and $\theta_{b,b'}$ denotes the elevation angle measured between the horizon and the line connecting user b to BS b'. In addition, $\psi_{b'}$ represents the fixed orientation angle of BS b' array boresight relative to the x-axis, while $\beta_{b'}$ denotes the *common* tilt applied to all the antennas of BS b' and is measured between the horizon and the line passing through the beam peak. A schematic illustration of the spherical angles is shown in Fig. 1. Moreover, $\mathrm{SLL}_{\mathsf{az}} = 25$ dB and $\mathrm{SLL}_{\mathsf{el}} = 17$ dB are the azimuth and elevation side lobe levels, respectively. $\phi^{\mathsf{3dB}}_{b'} = 65°$ and $\theta^{\mathsf{3dB}}_{b'} = 6°$ respectively denote the azimuth and elevation half power beamwidth of each antenna pattern.

C. Signal Model

Following the assumed propagation environment and antenna configuration, the channel vector between *active* user b and BS b', $b, b' \in \{1, \ldots, B\}$, can be expressed as $\alpha_{b,b'}(\beta_{b'})\boldsymbol{h}_{b,b'}$. Here, $\alpha_{b,b'}(\beta_{b'})$ is the path gain given by

$$\alpha_{b,b'}(\beta_{b'}) = \mathrm{L}_{b,b'} G_{b,b'}(\beta_{b'}), \quad (2)$$

where $\mathrm{L}_{b,b'}$ captures the pathloss between user b and BS b' and $G_{b,b'}(\beta_{b'}) = 10^{G^{\mathsf{dBi}}_{b,b'}(\beta_{b'})/10}$. In addition, $\boldsymbol{h}_{b,b'} \in \mathcal{C}^{N_{\mathsf{h}}\times 1}$ denotes the small-scale channel vector between user b and the N_{h} antennas at BS b' with the elements that are i.i.d. $\mathcal{CN}(0,1)$. We consider a narrowband frequency-flat channel and universal frequency reuse. The complex base-band received signal at user b is written as

$$y_b = \sum_{b'=1}^{B} \sqrt{\alpha_{b,b'}(\beta_{b'})}\, \boldsymbol{h}^{\mathsf{H}}_{b,b'} \boldsymbol{x}_{b'} + n_b, \quad (3)$$

where $\boldsymbol{x}_{b'} \in \mathcal{C}^{N_{\mathsf{h}}\times 1}$ is the transmitted signal from BS b', which is subject to a power constraint $\mathbb{E}[\boldsymbol{x}^{\mathsf{H}}_{b'}\boldsymbol{x}_{b'}] = P$, and n_b is the normalized additive white Gaussian noise distributed as $\mathcal{CN}(0,1)$. The transmit signal $\boldsymbol{x}_b$ is further expressed as $\boldsymbol{x}_b = \boldsymbol{w}_b d_b$, where $\boldsymbol{w}_b \in \mathbb{C}^{N_{\mathsf{h}}\times 1}$ and d_b denote respectively the unit-norm beamformer and the data symbol for user b.

III. Coordinated Transmission Strategy

In this section, we propose a novel coordination architecture in which the ICI is controlled in the elevation domain via coordinatively adapting the tilts of the BSs. In the azimuth domain, we use the intracell maximum ratio transmission (MRT) at the N_{h} antennas of each BS by setting $\boldsymbol{w}_b = \boldsymbol{h}_{b,b}/\|\boldsymbol{h}_{b,b}\|$ to maximize the desired signal power at the active user. Our coordination architecture includes the following components:

1) A division of the area of cell b, $\forall b$, into two vertical regions: i) a cell-interior region obtained as the intersection of cell b with a circle of radius r_b centered at BS b; ii) a cell-edge region obtained by removing the cell-interior region from cell b. This is illustrated in Fig. 2.

2) B different *coordinated transmission patterns* out of which one will be active at each time-slot. We index the patterns as $p = 1, \ldots, B$, where in pattern $p = b$, BS b serves its cell-edge region using β^p_b. BS b', $\forall b' \neq b$, however, coordinatively serves its cell-interior region by using $\beta^p_{b'} > \beta^p_b$ to decrease the ICI it causes to the cell-edge region of cell b. Each of the three vertical regions that are served in an active pattern is called the *active* region of its corresponding cell in that pattern. For example, in pattern $p = b$, cell-edge region

is the active region of cell b, while the cell-interior region is the active region of cell b', $\forall b' \neq b$.

3) A scheduler to dynamically share the time-slots between different coordinated transmission patterns. We define the activity factor of coordinated transmission pattern p, denoted as the ν_p ($0 \leq \nu_p \leq 1$), as the fraction of the time-slots over which it is active. The factors $\{\nu_p\}_{p=1}^{B}$ for any particular realization of K_b user locations in cell b, $\forall b$, depend on the number of users associated with different vertical regions and hence are denoted as *user-specific parameters*.

IV. Coordination Architecture Parameters

In this section, we determine the parameters of the proposed coordination architecture, i.e., $\{r_b\}_{b=1}^{B}$, $\{\beta_b^p\}_{\forall b,p}$ and $\{\nu_p\}_{p=1}^{B}$. The parameters $\{r_b\}_{b=1}^{B}$ and $\{\beta_b^p\}_{\forall b,p}$ are *by design* determined independently of the particular realization of users' locations in each vertical region, and hence are denoted as *region-specific parameters*. We emphasize that dynamic adaptation of the region-specific parameters to the particular realization of the users' locations can further improve the performance. Such adaptation, however, requires e.g., extensive channel quality measurements over candidate tilts and hence results in signaling overhead and complexity.

A. Region-Specific Parameters

To determine $\{r_b\}_{b=1}^{B}$ and $\{\beta_b^p\}_{\forall b,p}$, we focus on mean throughput maximization. Note that in the proposed coordination architecture the ICI to the users in the cell-edge region is sufficiently suppressed through the coordinated tilt adaptation applied in the neighboring cells. Thus, we expect the cell-edge user throughput to be at a satisfactory level for appropriate choices of regions-specific parameters that would maximize the mean throughput, as will be verified by simulation.

We first define the achievable throughput of an active user b located in the vertical region s of cell b as

$$R_b^s = \mathbb{E}_{p_s,\boldsymbol{h}}\left[\log_2\left(1+\frac{\alpha_{b,b}(\beta_b^{p_s})\|\boldsymbol{h}_{b,b}^{\mathsf{H}}\boldsymbol{w}_b\|^2 P}{1+\sum_{b'\neq b}\alpha_{b,b'}(\beta_{b'}^{p_s})\|\boldsymbol{h}_{b,b'}^{\mathsf{H}}\boldsymbol{w}_{b'}\|^2 P}\right)\right], \tag{4}$$

where the expectation is taken with respect to both p_s, denoting the patterns over which the vertical region s is active, and the small-scale fading. Without loss of generality, hereafter we focus on the symmetric network in Fig. 1, where we expect the region-specific parameters to be the same at all cells. To simplify the notation, we denote $r_b = r_{\text{int}}$, $\forall b$, $\beta_b^p = \beta^{\text{ci}}$, $\forall p, b$ where $p \neq b$, and $\beta_b^p = \beta^{\text{ce}}$, $\forall p, b$ where $p = b$.

Because we assume a uniform user distribution over the cell area, each user should be able to associate with either of the vertical regions with equal probability. Therefore, a reasonable choice is to set r_{int} such that the areas of the cell-interior region and cell-edge region are equal. With this criteria, after some geometrical calculation, we get $r_{\text{int}} \approx 0.65r$, where r is the cell radius defined as the distance from the BS to one of the vertices of the romb-shaped cell. Now, we need to determine the optimal values of β^{ci} and β^{ce} that maximizes the mean throughput. The authors in [11] have derived analytical

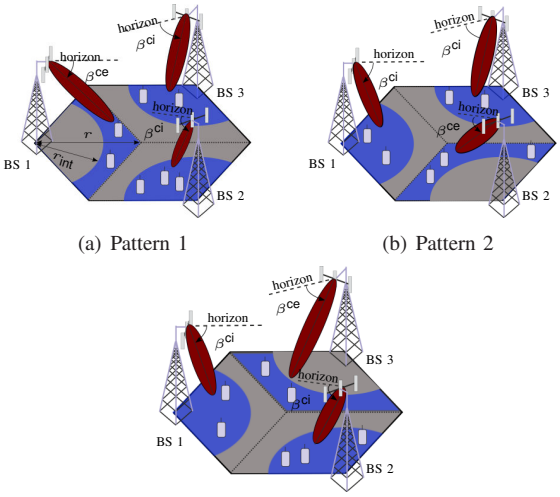

Fig. 2. Schematic illustration of the three coordinated transmission patterns in the proposed coordination architecture.

expressions for the optimal β^{ci} and β^{ce} in an isolated cell. In the presence of ICI, however, developing such analytical expressions becomes tedious if not impossible. Here, for simplicity we resort to a so-called throughput analysis. In this method, we first discretize the two vertical regions in each cell into a fine regular grid of user locations. Then for a given β^{ci} and β^{ce}, we compute the achievable throughput at each user location given in (4) by using the analytical expressions derived in [6]. The mean throughput can then be calculated readily using the cell throughput cumulative distribution function (CDF), which is obtained by concatenating the throughput values at both regions. To find the optimal values for β^{ci} and β^{ce}, we exhaustively search over $\left[\arctan(\frac{h_{\text{bs}}-h_{\text{u}}}{r_{\text{int}}}), 90°\right]$ for β^{ci} and over $\left[0°, \arctan(\frac{h_{\text{bs}}-h_{\text{u}}}{r_{\text{int}}})\right]$ for β^{ce} to find the ordered pair $(\beta^{\text{ci}}_{\text{opt}}, \beta^{\text{ce}}_{\text{opt}})$ that maximizes the mean throughput.

Our simulation parameters are as follows. We set $r = 288.6751$ m, corresponding to an inter-site distance of 500 m in 3GPP case 1 [10], $h_{\text{bs}} = 32$ m, $h_{\text{u}} = 1.5$ m, and $N_{\text{h}} = 4$. The pathloss factor $\text{L}_{b,b'}$ is given in dB by $-(128.1 + 37.6\log_{10}(d_{b,b'}))$, where $d_{b,b'}$ denotes the distance (in km) between user b and BS b' accounting for the BS and the user heights [6]. Furthermore, the transmit power P is set such that the cell-edge SNR, defined as the SNR experienced at the edge of an isolated cell excluding the effect of antenna gain, is 10 dB. We found that the maximum mean throughput is achieved by using $\beta^{\text{ci}}_{\text{opt}} = 13.7°$ and $\beta^{\text{ce}}_{\text{opt}} = 8.3°$.

B. User-Specific Parameters

We define $\mathcal{K}_b$ to be the set of users in cell b such that $|\mathcal{K}_b| = K_b$. We further define $\mathcal{K}_b^{\text{ci}} \subset \mathcal{K}_b$ and $\mathcal{K}_b^{\text{ce}} \subset \mathcal{K}_b$ to be respectively the sets of users associated with BS b in the cell-interior region and cell-edge region such that $\mathcal{K}_b^{\text{ci}} \bigcap \mathcal{K}_b^{\text{ce}} = \emptyset$, and $\mathcal{K}_b^{\text{ci}} \bigcup \mathcal{K}_b^{\text{ce}} = \mathcal{K}_b$. We focus on one drop of $|\mathcal{K}_b^{\text{ci}}| + |\mathcal{K}_b^{\text{ce}}|$ users in cell b, $\forall b$. Now, to determine $\{\nu_b\}_{b=1}^{B}$ we need to solve the following optimization problem:

$$\begin{aligned} &\text{maximize} \quad g(\boldsymbol{R}) \\ &\text{subject to} \quad R_k \leq \begin{cases} (1-\nu_b)R_{k,\text{sch}}^{\text{ci}} & \text{if } k \in \mathcal{K}_b^{\text{ci}} \\ \nu_b R_{k,\text{sch}}^{\text{ce}} & \text{if } k \in \mathcal{K}_b^{\text{ce}} \end{cases}, \end{aligned}$$

$$\sum_{b=1}^{B} \nu_b = 1, \nu_b \geq 0. \tag{5}$$

In (5), $g(\cdot)$ denotes some desired utility function, R_k denotes the achievable throughput of user k, and $\boldsymbol{R}$ denotes the vector of achievable throughput of all users in the coverage area. In addition, $R^{\mathsf{ci}}_{k,\mathsf{sch}}$ and $R^{\mathsf{ce}}_{k,\mathsf{sch}}$ indicate the *per region throughput* for user k in the cell-interior region and cell-edge region, respectively. $R^{\mathsf{ci}}_{k,\mathsf{sch}}$ ($R^{\mathsf{ce}}_{k,\mathsf{sch}}$) is obtained by averaging the instantaneous rate over all the time-slots in which the cell-interior region (cell-edge region) is active. Note that user $k \in \mathcal{K}^{\mathsf{ci}}_b$ ($k \in \mathcal{K}^{\mathsf{ce}}_b$) might not necessarily be served at each time-slot in which the cell-interior region (cell-edge region) of cell b is active, in which case its instantaneous rate is zero. Therefore, $R^{\mathsf{ci}}_{k,\mathsf{sch}}$ ($R^{\mathsf{ce}}_{k,\mathsf{sch}}$) is in general different from (4).

In this paper, we focus on the popular case of proportional fairness scheduling (PFS) with $g(\boldsymbol{R}) = \sum_{b=1}^{B} \sum_{k \in \mathcal{K}_b} \log_2(R_k)$. Solving Karush-Kuhn-Tucker (KKT) conditions for (5) under PFS, ν_b is obtained as

$$\nu_b = \frac{\mu + |\mathcal{K}_b| - \sqrt{(\mu + |\mathcal{K}_b|)^2 - 4\mu|\mathcal{K}^{\mathsf{ce}}_b|}}{2\mu}, \tag{6}$$

where μ is that solution of the fixed-point equation

$$\mu = \sum_{b=1}^{B} \sqrt{(\mu + |\mathcal{K}_b|)^2 - 4\mu|\mathcal{K}^{\mathsf{ce}}_b|} - |\mathcal{K}_b|, \tag{7}$$

for which we have $\sum_{b=1}^{B} \nu_b = 1$. We highlight that for the PFS utility function the activity factor ν_b, $\forall b$, is independent of $R^{\mathsf{ci}}_{k,\mathsf{sch}}$ and $R^{\mathsf{ce}}_{k,\mathsf{sch}}$, $\forall k \in \mathcal{K}_b$, which might not be the case for other utility functions. Solving (5) for a general utility function is a topic for future work.

We finally remark that for any given number of users K_b in cell b, $\forall b$, the activity factor of pattern b, ν_b, is a discrete random variable whose value depends on the particular realization of K_b users' locations in cell b, $\forall b$. Figure 3 shows the normalized histogram (probability mass function) of the activity factor of pattern 1 (ν_1) obtained from 1000 drops of $K_1 = K_2 = K_3 = 10$ users in the network of Fig. 1. The activity factor for each drop is calculated using 6. It can be seen that ν_1 can take different values over the range $(0, 1)$, which emphasizes the importance of dynamic allocation of time (or frequency) resources to the particular realization of users' locations in each vertical region.

V. Numerical Results

In this section, we evaluate the performance of the proposed coordinated transmission strategy using Monte Carlo simulation. Our simulations parameters follow those in Section IV-A. We use a drop-based simulation, where at each drop 10 users are randomly placed in each romb-shaped cell. The users in each cell are associated with the cell-interior region or the cell-edge region based on their locations. The time-slots are dynamically shared among the vertical regions according to (6). The users in each vertical region are served using standard PFS. We simulate a sufficient number of small-scale fading realizations such that all users achieve their limiting

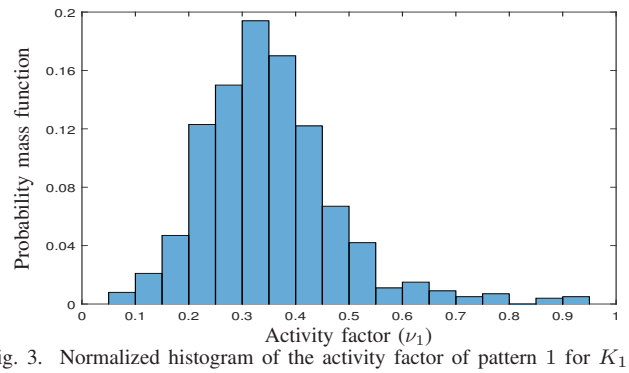

Fig. 3. Normalized histogram of the activity factor of pattern 1 for $K_1 = K_2 = K_3 = 10$.

throughputs. The users' throughput over all drops are then stacked to obtain the throughput CDF over the cell area.

We compare the performance of five different transmission strategies: 1) an uncoordinated transmission strategy based on intracell MRT and cell-specific tilting (CST) [11] with a mean-throughput maximizing tilt 13° applied at all BSs, denoted as MRT-CST; 2) the proposed coordinated transmission strategy with intracell MRT, coordinated region-specific tilting (CRST), and dynamic resource allocation, denoted as MRT-CRST-DRA; 3) the transmission strategy in 2), but with static resource allocation, i.e., by setting $\nu_1 = \nu_2 = \nu_3 = 1/3$, denoted as MRT-CRST-SRA; 4) an uncoordinated transmission strategy based on intracell MRT and user-specific tilting (UST) [11], denoted as MRT-UST. In this strategy, each BS assumes a common fixed tilt of 13° at the other BSs at the scheduling stage as it does not know which users they will serve. The final rate of the users is, however, calculated based on the actual applied tilts at the BSs; and 4) a coordinated transmission strategy based on CSI-aware ICI cancellation (ICIC) [11] and CST with a mean-throughput maximizing tilt of 9° applied at all BSs, denoted as ICIC-CST. In this strategy, the scheduling at each BS is performed assuming intracell MRT and no ICI. Once the active user is selected in each cell, BSs exchange the necessary CSI and update their beamformers to null the ICI to the active users in the neighboring cells.

Figure 4 compares the throughput CDF for different transmission strategies. As can be seen, the MRT-CRST-DRA significantly improves the user throughput compared to MRT-CST over the cell area except at regions in the middle of the cell (indicated by throughput values around 50-percentile of the throughput CDF). Compared to MRT-CRST-SRA, the proposed technique enhances the performance only in the outer part of the cell (represented by lower portion of the throughput CDF). It is also observed that MRT-UST has superior performance compared to MRT-CRST-DRA over a large part of the cell area except at regions close to the BS (indicated by upper portion of the CDF curve). It seems that for users close to the BSs, the desired signal power gain brought by pointing the peak of the main beam towards the user in MRT-UST to be less than the loss due to ICI caused by uncoordinated UST at the neighboring BSs. Finally, it is observed that MRT-CRST-DRA has inferior performance to ICIC-CST in the outer part of the cell (represented by lower portion of the throughput CDF), while it has a superior performance than ICIC-CST in

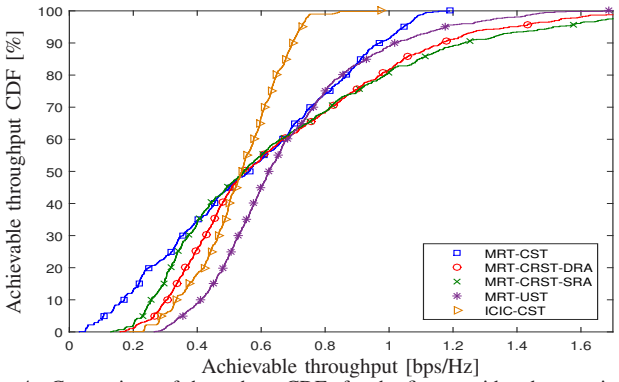

Fig. 4. Comparison of throughput CDFs for the five considered transmission strategies.

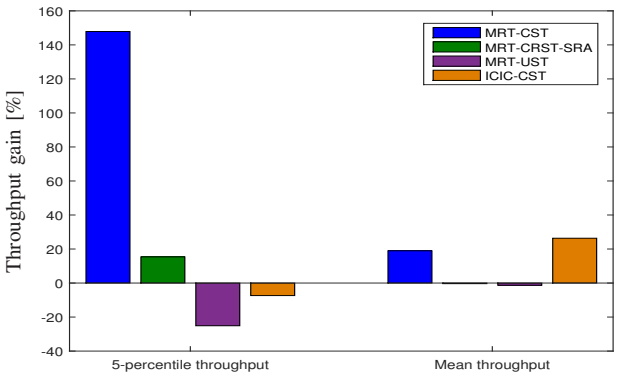

Fig. 5. Performance gain of the proposed scheme over the other four comparative transmission strategies.

the inner part of the cell (indicated by the upper portion of the CDF curve). This is because for the users close to the BSs, the desired signal power loss at the home BS due to ICIC to neighboring cells is usually larger than the ICI cancellation gain brought by the neighboring BSs.

Figure 5 shows the 5-percentile throughput, denoted as the edge throughput, and mean throughput gain of MRT-CRST-DRA over the other four comparative transmission strategies. The gain over MRT-CST comes from desired signal power improvement because of tilt adaptation and ICI suppression achieved by serving non-adjacent vertical regions in each transmission pattern. The edge throughput gain compared to MRT-CRST-SRA is due to dynamic allocation of time-slots among different patterns. In fact, with dynamic resource allocation, the patterns with a larger number of users in their corresponding active cell-edge regions will be served over more time-slots, resulting in an increased achievable throughput of the cell-edge users. The edge and mean throughput loss compared to MRT-UST is mainly because of desired signal power gain achieved by pointing the peak of the main beam towards the user in MRT-UST. The superior edge throughput of ICIC-CST compared to MRT-CRST-DRA is because it completely cancels ICI. The mean throughput loss of ICIC-CST is attributed to its worse performance in the cell interior region. Note that the provided performance of both MRT-UST and ICIC-CST are optimistic. For MRT-UST, we consider an infeasible BS tilting capability of changing the tilt from 0° to 90°. For ICIC-CST, we assumed perfect CSI exchange among BSs that would not be possible in practice due to backhaul delay, error, etc. [4]. Therefore, we expect the aforementioned performance differences to be even less in practice.

Finally, we highlight that in the MRT-CRST-DRA (and MRT-CRST-SRA) one vertical region will be active at each time-slot. Hence, only users in the active vertical region in each cell need to provide detailed CSI feedback to their home BS at each time-slot instead of all users in the cell as in the other comparative techniques. Since the area of each vertical region is half of the cell area, this results in 50% signaling overhead reduction on average.

VI. Concluding Remarks

In this paper, we proposed a novel coordinated transmission strategy that exploits the elevation plane of the wireless channel for ICI management in cellular networks. The key idea is to divide the cell area into two vertical regions and to serve non-adjacent vertical regions in neighboring cells according to predetermined patterns and by applying practical tilts at the BSs. The proposed transmission strategy achieves significant edge throughput gain over conventional uncoordinated transmission and shows comparable performance to schemes assuming CSI sharing or infeasible BS tilting capabilities. It requires no CSI sharing among the BSs, and also reduces the intracell feedback by about 50% on average.

We highlight that the promised performance gain of the proposed coordinated transmission strategy might decrease when applied to networks with a large number of cells. This is because the activity factor of the cell-edge region in such networks might become small as only one cell can serve its cell-edge region at each time-slot. Future research should investigate other techniques such as dynamic or static clustering to utilize the proposed technique in large networks.

References

[1] J. G. Andrews and *et al.*, "What will 5G be?" *IEEE J. Sel. Areas Commun.*,, vol. 32, no. 6, pp. 1065–1082, Jun. 2014.

[2] R. Irmer and et al., "Coordinated multipoint: Concepts, performance, and field trial results," *IEEE Commun. Mag.*, vol. 49, no. 2, pp. 102–111, february 2011.

[3] J. Zhang and J. Andrews, "Adaptive spatial intercell interference cancellation in multicell wireless networks," *IEEE J. Sel. Areas Commun.*, vol. 28, no. 9, pp. 1455–1468, Dec. 2010.

[4] N. Seifi, J. Zhang, R. W. Heath Jr., T. Svensson, and M. Coldrey, "Coordinated 3D beamforming for interference management in cellular networks," *IEEE Trans. Wireless Commun.*, vol. 13, no. 10, pp. 5396–5410, Oct. 2014.

[5] L. Thiele and *et al.*, "Modeling of 3D field patterns of downtilted antennas and their impact on cellular systems," in *Int. ITG WSA*, Berlin, Germany, Feb. 2009.

[6] N. Seifi, M. Coldrey, and M. Viberg, "Throughput optimization for MISO interference channels via coordinated user-specific tilting," *IEEE Commun. Letters*, vol. 16, no. 8, pp. 1248–1251, Aug. 2012.

[7] N. Gresset, H. Halbauer, J. Koppenborg, W. Zirwas, and H. Khanfir, "Interference-avoidance techniques: Improving ubiquitous user experience," *IEEE Veh. Technol. Mag.*, vol. 7, no. 4, pp. 37–45, Dec. 2012.

[8] H. Halbauer, S. Saur, J. Koppenborg, and C. Hoek, "3d beamforming: Performance improvement for cellular networks," *Bell Labs Technical Journal*, vol. 18, no. 2, pp. 37–56, 2013. [Online]. Available: http://dx.doi.org/10.1002/bltj.21604

[9] H. Halbuer, J. Koppenborg, J. Holfeld, M. Danneberg, M. Grieger, and G. Fettweis, "Field trial evaluation of 3D beamforming in a multicell scenario," in *Int. Wrkshp Smart Ant. (WSA)*, Stuttgart, Germany, 2013.

[10] G. T. . V9.0, "Further advancements for E-UTRA physical layer aspects," Tech. Rep., Mar. 2010.

[11] W. Lee, S. R. Lee, H. B. Kong, S. Lee, and I. Lee, "Downlink vertical beamforming designs for active antenna systems," *IEEE Trans. Commun.*, vol. 62, no. 6, pp. 1897–1907, Jun. 2014.